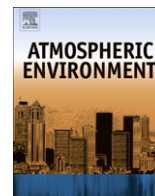




Contents lists available at ScienceDirect

## Atmospheric Environment

journal homepage: [www.elsevier.com/locate/atmosenv](http://www.elsevier.com/locate/atmosenv)

## Impact of the 2009 Attica wild fires on the air quality in urban Athens

V. Amiridis<sup>a,\*</sup>, C. Zerefos<sup>b,c</sup>, S. Kazadzis<sup>d</sup>, E. Gerasopoulos<sup>d</sup>, K. Eleftheratos<sup>b,c</sup>, M. Vrekoussis<sup>b,e</sup>, A. Stohl<sup>f</sup>, R.E. Mamouri<sup>a,g</sup>, P. Kokkalis<sup>g</sup>, A. Papayannis<sup>g</sup>, K. Eleftheriadis<sup>h</sup>, E. Diapouli<sup>h</sup>, I. Keramitsoglou<sup>a</sup>, C. Kontoes<sup>a</sup>, V. Kotroni<sup>d</sup>, K. Lagouvardos<sup>d</sup>, E. Marinou<sup>a</sup>, E. Giannakaki<sup>i</sup>, E. Kostopoulou<sup>d</sup>, C. Giannakopoulos<sup>d</sup>, A. Richter<sup>e</sup>, J.P. Burrows<sup>e</sup>, N. Mihalopoulos<sup>j</sup>

<sup>a</sup>Institute for Space Applications and Remote Sensing, National Observatory of Athens, I. Metaxa & Vas. Pavlou str., GR-15236 Penteli, Athens, Greece

<sup>b</sup>Biomedical Research Foundation, Academy of Athens, Athens, Greece

<sup>c</sup>Laboratory of Climatology and Atmospheric Environment, University of Athens, Athens, Greece

<sup>d</sup>Institute for Environmental Research and Sustainable Development, National Observatory of Athens, Athens, Greece

<sup>e</sup>Institute of Environmental Physics and Remote Sensing, University of Bremen, Bremen, Germany

<sup>f</sup>Norwegian Institute for Air Research, Kjeller, Norway

<sup>g</sup>Physics Department, National Technical University of Athens, Athens, Greece

<sup>h</sup>Environmental Radioactivity Laboratory, National Centre of Scientific Research Demokritos, Athens, Greece

<sup>i</sup>Laboratory of Atmospheric Physics, Aristotle University of Thessaloniki, Thessaloniki, Greece

<sup>j</sup>Environmental Chemical Processes Laboratory, University of Crete, Heraklion, Greece

## ARTICLE INFO

## Article history:

Received 12 November 2010

Received in revised form

20 July 2011

Accepted 27 July 2011

## Keywords:

Pollution

Biomass burning

Aerosol

Photochemistry

Radiation

## ABSTRACT

At the end of August 2009, wild fires ravaged the north-eastern fringes of Athens destroying invaluable forest wealth of the Greek capital. In this work, the impact of these fires on the air quality of Athens and surface radiation levels is examined. Satellite imagery, smoke dispersion modeling and meteorological data confirm the advection of smoke under cloud-free conditions over the city of Athens. Lidar measurements showed that the smoke plume dispersed in the free troposphere and lofted over the city reaching heights between 2 and 4 km. Ground-based sunphotometric measurements showed extreme aerosol optical depth, reaching nearly 6 in the UV wavelength range, accompanied by a reduction up to 70% of solar irradiance at ground. The intensive aerosol optical properties, namely the Ångström exponent, the lidar ratio, and the single scattering albedo, showed typical values for highly absorbing fresh smoke particles. In-situ air quality measurements revealed the impact of the smoke plume down to the surface with a slight delay on both the particulate and gaseous phase. Surface aerosols increase was encountered mainly in the fine mode with prominent elevation of OC and EC levels. Photochemical processes, studied via NO<sub>x</sub> titration of O<sub>3</sub>, were also shown to be different compared to typical urban photochemistry.

© 2011 Elsevier Ltd. All rights reserved.

## 1. Introduction

Biomass burning is a significant source of gases and particulates both at regional and global scales, having significant radiative effects and subsequent climate impacts (e.g. Crutzen and Andreae, 1990). According to IPCC-AR4 (Forster et al., 2007), smoke has a contribution of roughly  $+0.04 \pm 0.07 \text{ W m}^{-2}$  to the global radiative forcing. This impact has been the subject of particular interest since the extent of biomass burning increased significantly over the

past 100 years, and is currently recognized as a significant global source.

Southern Europe is a fire-prone area, expected to be even more affected by wild fires in the future. Future scenarios on climate change indicate that the already hot and semi-arid climate of southern Europe is expected to become warmer and drier and such climate conditions may trigger increased fire occurrence (Giannakopoulos et al., 2009, 2011). Greece in particular, faces a severe threat from forest fires, which is evident from the number of fires that break out every year. Especially for the Attica peninsula, the MODIS active fire product recorded around 2000 instances during the last decade, mainly in August and July. Two maxima were identified, one in 2007 (27% of the fires in the decade), attributed to the exceptionally hot and dry conditions during that

\* Corresponding author. Tel.: +30 2108109116; fax: +30 2106138343.

E-mail address: [vamoir@noa.gr](mailto:vamoir@noa.gr) (V. Amiridis).

URL: <http://www.space.noa.gr/>

summer (Founda and Giannakopoulos, 2009); and one in 2009 (23% of the fires in the decade).

Recent studies demonstrate the significant role of biomass burning aerosols in the Eastern Mediterranean (e.g. Sciare et al., 2008), with negative surface radiative forcing and large positive atmospheric forcing values, nearly identical to the highly absorbing south Asian haze over the Arabian Sea (Markowicz et al., 2002). Only few studies demonstrate the smoke impact on the air quality and radiation over Greece and most of them are concentrated to the advection of air masses from fires in Southern Eastern Europe (Balis et al., 2003; Amiridis et al., 2005; Kazadzis et al., 2007; Amiridis et al., 2009a,b; Sciare et al., 2008; Gerasopoulos et al., 2011), or those during summer 2007 in Peloponnese peninsula (Liu et al., 2009; Turquetly et al., 2009). In the first case, the studies report on the effect of aged smoke on long-term ground-based measurements, while in the second case, the evolution of the smoke plume is described, based on satellite observations. At a climatological basis, Karanasiou et al. (2009), reports that aerosol PM<sub>10</sub> mass concentrations in Athens are regularly affected by biomass burning with a mean contribution ranging from 7 to 9%. However, none of the aforementioned studies has put insight on the impact of fresh smoke from local fires, on the background air pollution levels of an urban environment.

In addition to the direct fire damage, the 2009 fires in the Attica peninsula degraded the air quality of the urban Athens area, due to large quantities of gaseous air pollutants and particles emitted. In this study, the 2009 fires near the city of Athens and their impact on urban air quality and surface radiation fields are investigated.

## 2. Data and methodology

### 2.1. Surface radiation and aerosol columnar properties

Since February 2009, the National Observatory of Athens (NOA/ISARS) is continuously operating the ground-based Atmospheric Remote Sensing Station (ARSS), to monitor radiation levels at ground and aerosol loadings over the city of Athens (Amiridis et al., 2009a,b). ARSS is located on the roof of the Biomedical Research Foundation of the Academy of Athens (BRFAA, 37.9°N, 23.8°E, 130 m a.s.l.). ARSS is equipped with a CIMEL sunphotometer and a UV-MFR radiometer. In addition, a Brewer MKIV monochromator operates since June 2003 (Zerefos and Eleftheratos, 2007). The UV-MFR is used to measure both total and diffuse irradiance at seven specified wavelengths (from 300 to 368 nm). The Brewer spectroradiometer is used to measure the erythemal irradiance during the event.

Measurements of the aerosol optical depth (AOD) at 8 wavelengths from 340 to 1640 nm are performed at ARSS using the CIMEL sunphotometer (as part of NASA's AERONET, Aerosol Robotic Network, <http://aeronet.gsfc.nasa.gov>). The technical specifications of the instrument are given in detail by Holben et al. (1998). Additional AODs have been retrieved from the UV-MFR by means of Langley plot analysis (Harrison and Michalsky, 1994).

### 2.2. Aerosol vertical distribution

The NTUA (National Technical University of Athens) 6-wavelength Raman lidar system is used to perform measurements of the aerosol vertical structure in the free troposphere (Mamouri et al., 2009), at a horizontal distance of 400 m from ARSS. The measurement of the elastic-backscatter signal at 355 and 532 nm, as well as that of the N<sub>2</sub> inelastic-backscatter signals at 387 and 607 nm, permit the determination of the extinction and backscatter coefficients, from which the extinction-to-backscatter ratio (lidar ratio - LR) at both wavelengths (355 and 532 nm) is calculated. Quality assurance both at hardware (Matthias et al., 2004) and algorithm (Pappalardo et al.,

2004) level, is assured within the frame of the European Aerosol Lidar Network (EARLINET).

### 2.3. Aerosol and air pollutants at surface

Measurements of aerosol physicochemical properties during the fire were available from the GAW Regional NCSR Demokritos station, DEM 38.0°N 23.8°E (270 m a.s.l.), operating in the periphery of the Athens Metropolitan Urban area. Black carbon (BC) concentrations were obtained by a seven wavelength AE-31 Aethalometer (Maggee Sci.) and were used as a surrogate parameter for the mass associated with light absorbing aerosol. Elemental and Organic Carbon (EC and OC) concentrations were obtained by a Thermo-optical analyzer (Sunset Labs) on PM<sub>2.5</sub> prefired Quartz filter samples, the total mass of which obtained by gravimetric analysis.

Additional nitrogen oxides (NO<sub>x</sub>), surface ozone (O<sub>3</sub>) and particulate matter (PM<sub>2.5</sub> and PM<sub>10</sub>) concentrations, at five sites in the Greater Athens Area (GAA), were used (Fig. 1). NO<sub>x</sub> and O<sub>3</sub> concentrations were provided on an hourly basis, whereas PM data were available on a daily basis. Detailed description of the sites and instrumentation can be found in Grivas et al. (2008).

### 2.4. Synergistic measurements and modeling tools

MODIS active fire product (Giglio et al., 2003) was used to identify the fire locations and the smoke emissions needed for dispersion modeling. To estimate the total burnt area from the fires, Burn Scar Mapping (BSM) has been carried out within the framework of SAFER (Services and Applications for Emergency Response) GMES project, using Landsat-TM images (Kontoes, 2008). The method has been intensively used and operationally validated over Greece, in the framework of the RISK-EOS project ([www.riskeos.com](http://www.riskeos.com)).

To simulate transport processes, we employed the Lagrangian particle dispersion model FLEXPART (Stohl et al., 2005, 2007). The model is driven by operational analysis data from the ECMWF model. Following Seiler and Crutzen (1980), the emissions of carbon monoxide (CO) from the fires were estimated and used as a tracer for dispersion of the fire plume. Finally, satellite data from GOME-2 were used for the retrieval of NO<sub>2</sub> using the differential optical absorption spectroscopy, DOAS (e.g. Richter and Burrows, 2002).

## 3. Evolution of the fires and the smoke plume

### 3.1. Fire geographical extent

In August 2009, wild fires ravaged the north-eastern fringes of Athens, destroying great part of the capital's forests. The fire was ignited on August 21, about 40 km NE of Athens, and quickly intensified due to the prevailing strong North-eastern winds, that spread the major front of the flames toward Mount Penteli, during the following four days. Fig. 1 shows the burnt areas as identified using a Landsat-TM satellite image acquired on 12 of October 2009, soon after the 2009 fire season (left panel). These areas coincide with the fire incidences detected by MODIS in the time period between 20 and 25 of August 2009 (not shown). The BSM\_NOA methodology revealed a total burnt area of 13,045 ha. From that, 5786 ha were transitional woodland shrub. The rest were coniferous trees (470 ha), natural grassland (261 ha) and other land cover classes including urban and agricultural land (2468 ha). The figure also reveals that the large fires occurred in the wildland/urban interfaces (urban areas are represented in gray color). The locations of the stations used in this study are superimposed.

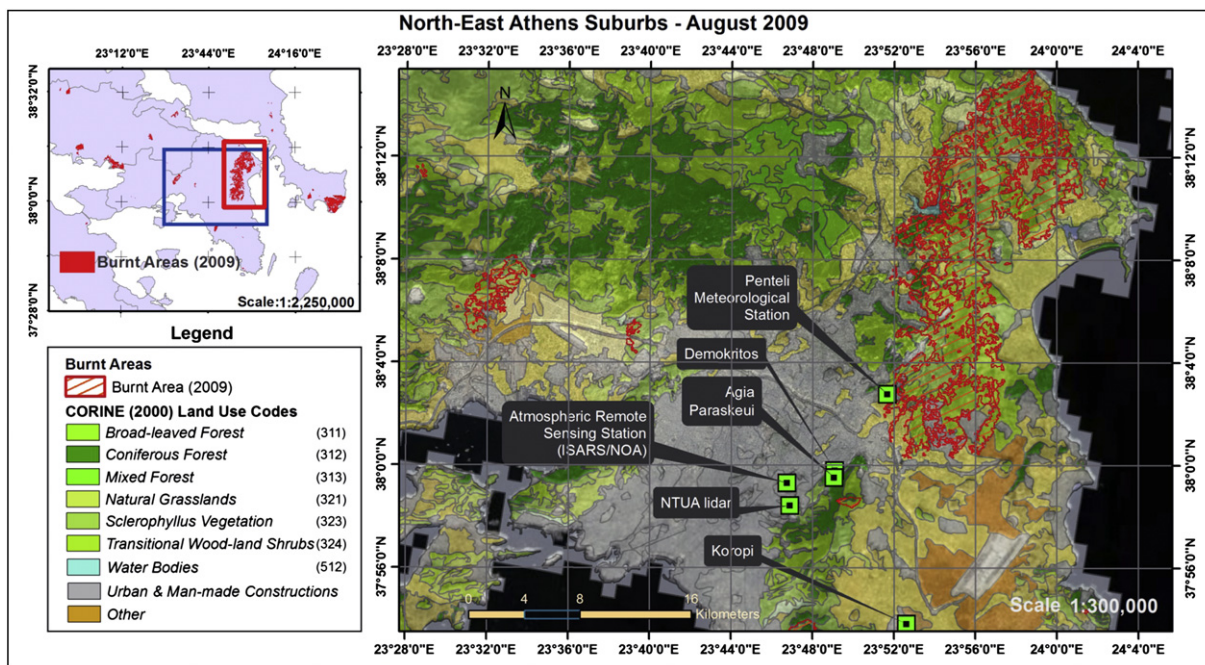


**Fig. 1.** Burnt areas identified by Burn Scar Mapping (BSM\_NOA) on Landsat images. BSM is overlaid on Corine Land Cover 2000. Source: SAFER project (Services and Applications For Emergency Response; GMES – FP7-SPACE-2007-001).

### 3.2. Smoke signature over GAA and advection over Athens

On August 21, an Etesian wind regime was established over Greece (Prezerakos, 1984). Fig. 2 (left panel) shows the maximum wind speed, as recorded at the surface meteorological station at Penteli (~500 m high in the north-eastern part of GAA). It is noteworthy that during the whole period the wind direction was from the northern sector with north-northwest being the prevailing direction (Fig. 2 - right panel). On August 21, wind speed exceeded  $10 \text{ m s}^{-1}$  with gusts over  $15 \text{ m s}^{-1}$ . On August 23, the northerly winds increased again to strong (04:00–10:00 UTC) with gusts that reached  $17.3 \text{ m s}^{-1}$  at 09:00 UTC. Measurements at different stations inside the GAA (not shown here) confirmed the described conditions. These findings support that during the early time of the forest fire, the conditions intensified the spread of the forest fire, while during the period 22–23 August the transport of the smoke plume toward the central part of the GAA and over the city of Athens was favored.

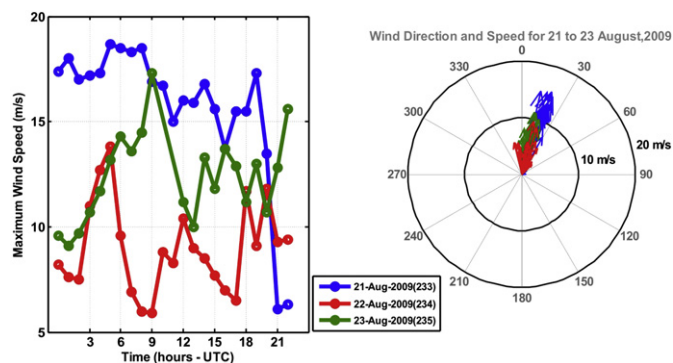


**Fig. 2.** Maximum wind speed (left panel) and mean wind speed and direction (right panel), at hourly time-intervals, as recorded at the surface meteorological station of Penteli.

The impact of the wild fires on air quality over GAA, on August 22–23 was well captured by GOME-2 observations of the tropospheric column amounts of  $\text{NO}_2$  (Fig. 3). Both days the  $\text{NO}_2$  plume coincides with the smoke plumes as seen by MODIS. During the peak of the wild fires, on August 22, the vertical column density was  $(9.9 \pm 4.0) \times 10^{15} \text{ molecules cm}^{-2}$ . The estimated uncertainty is the upper limit (80%) of the GOME-2 tropospheric column uncertainty reported for polluted conditions (Valks et al., 2011). The  $\text{NO}_2$  levels increased about 200% in comparison to the observed “background” levels of  $(3.05 \pm 0.91) \times 10^{15} \text{ molecules cm}^{-2}$ , computed for the previous and subsequent period ( $37.75^\circ\text{N}$ – $38.00^\circ\text{N}$ ,  $23.65^\circ\text{E}$ – $23.90^\circ\text{E}$ ), as well as to the mean August values for 2008 and 2010 ( $\approx 3.2 \times 10^{15} \text{ molecules cm}^{-2}$ ).

In addition to  $\text{NO}_2$  observations, CO tracer simulations by the FLEXPART dispersion model for August 22 and 23, at 10:00 UTC, are presented in Fig. 4 (upper panels). Three major smoke plumes are visible, related to the active fires in the region. We focus on the denser central plume which affected the city of Athens. The lower panels of Fig. 4 show the vertical sections of the CO tracer concentrations along the black line plotted in the upper panels. According to FLEXPART simulations, the CO tracer generated by the fires filled the boundary layer up to approximately 3 km a.s.l. near the source and over the city of Athens. Maximum CO concentrations are found to be up to  $400 \mu\text{g m}^{-3}$  along the central plume axis. During the entire transport along the Aegean Sea, the CO tracer remained below about 2–3 km, as vertical transport was capped by the anticyclonic subsidence.

## 4. Impact on air quality and surface radiation

### 4.1. Impact on columnar aerosol load: extensive and intensive properties

In Fig. 5, the time-height plot of lidar derived range-corrected backscatter signal at 1064 nm is presented for 21–25 August 2009. During the period of study significant values of the aerosol



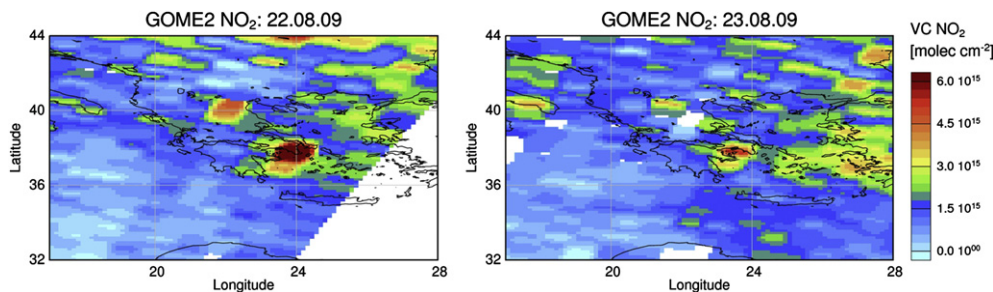


**Fig. 3.** GOME-2 Vertical Column Densities of  $\text{NO}_2$  over Greece. The highest values of  $\text{VCD}_{\text{NO}_2}$  (shown in red) were obtained on August 22 and 23. (For interpretation of the references to color in this figure legend, the reader is referred to the web version of this article.)

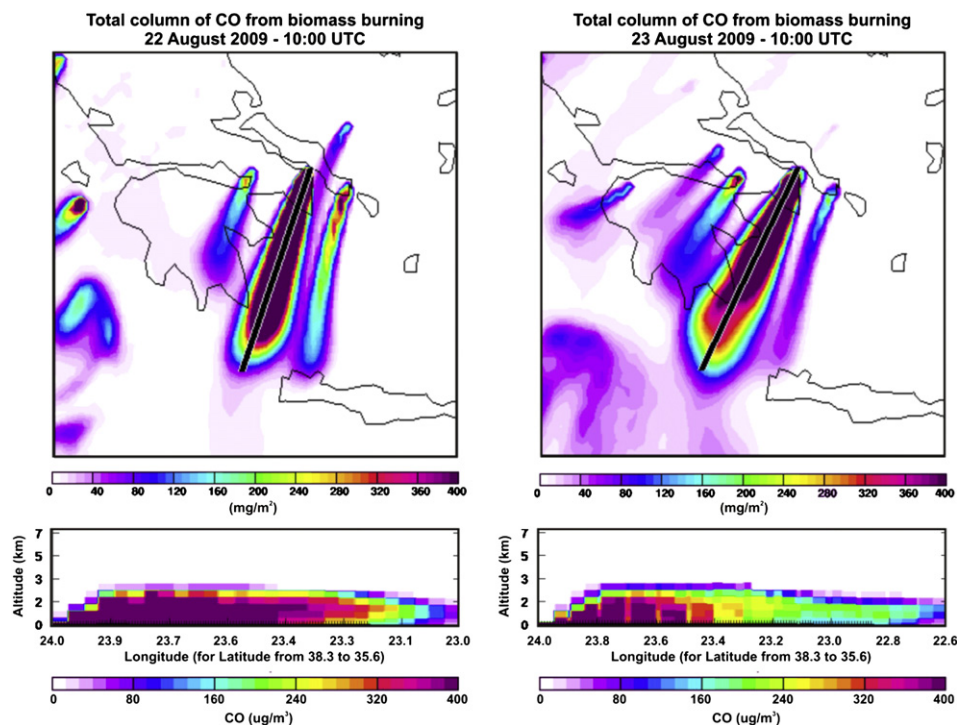


**Fig. 4.** FLEXPART simulations of CO concentrations from the fires as captured by MODIS. CO total column concentrations are presented on the upper panel for August, 22 (left) and 23 (right). Respectively, the vertical profiles of CO are presented in the lower panel for the black line indicated in the upper panel.

backscatter coefficients were found up to 3 km height. FLEXPART simulations of the smoke vertical transport found to be consistent with the lidar measurements. However, lidar measurements indicate that during August 22, the smoke plume reached heights also

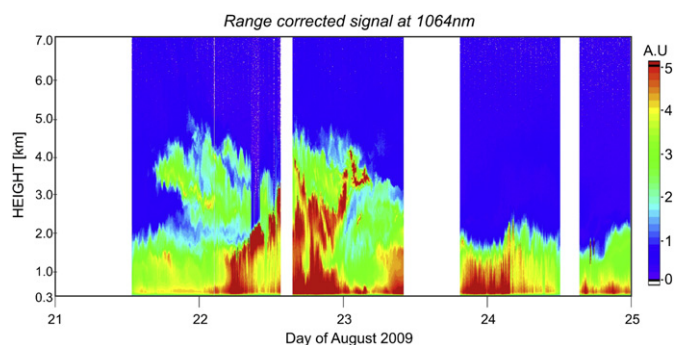


**Fig. 5.** Time-series of the range-corrected backscatter signal vertical distribution at 1064 nm (Arbitrary Units – A.U.) from 21 to 25 August 2009. The vertical and temporal resolution is of the order of 15 m and 90 s, respectively.

between 4 and 5 km. It is evident from Fig. 5 that the higher aerosol concentrations were recorded on August 22. August 23 also revealed high backscatter returns in relation to 21 and 24, however, the aerosol load was located in lower altitudes, most probably only within the planetary boundary layer.

AOD measurements at 368 nm from the UV-MFR (Fig. 6a), show extreme values, between 15:00 and 18:00 UTC in the afternoon of 22, and between 2:00 and 4:00 UTC during August 23. In addition, high AOD values were recorded for a limited time during August 21, resulting from another weaker fire in the south west of Athens. Co-located CIMEL measurements at 500 nm (Fig. 6b) show very high AODs as well for August 23. However, the cloud screening methodology, regularly applied in the CIMEL post production AOD calculation, lead to the elimination of a number of measurements during the intense smoke event (morning of the 22 and part of 23 of August, Fig. 6b – lower panel). From the available CIMEL measurements it is evident that the AODs recorded during the smoke episode were well above the climatological value of  $\text{AOD} = 0.23 \pm 0.09$  (black/dotted lines in Fig. 6b, lower panel). It is also evident that the aerosol fine mode strongly dominates over the coarse mode. The

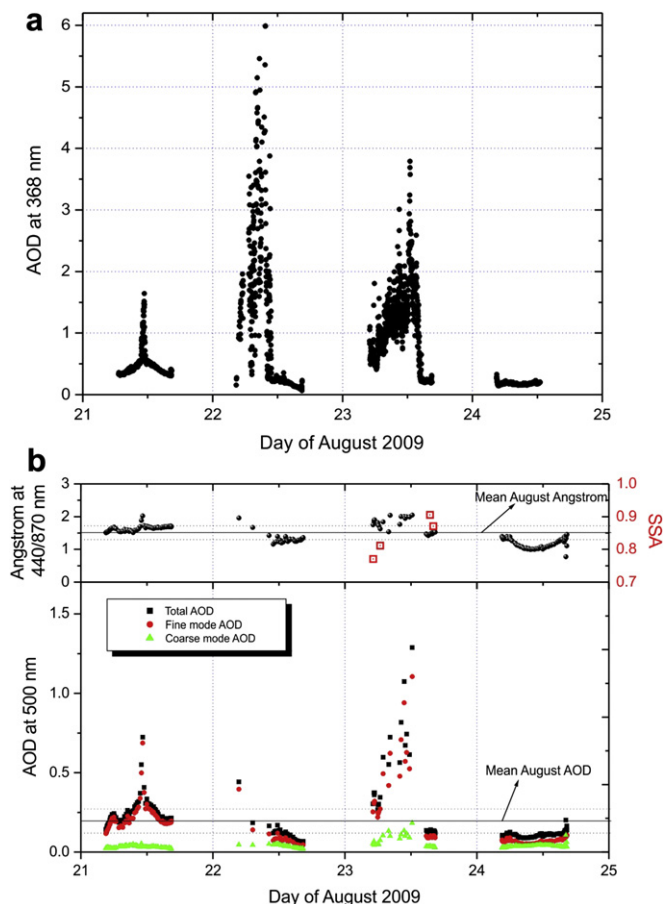


**Fig. 6.** (a) AOD measurements with the UV-MFR-SR at 368 nm, (b) Ångström exponent 440/870 nm (upper panel) and AOD measurements at 500 nm (lower panel) with the CIMEL. The black and dotted lines denote the mean climatological values for August and the corresponding standard deviation.

presence of fine particles is indicated also in the upper panel of Fig. 6b, which presents the 440/870 nm Ångström exponent, along with the mean climatological value of this parameter for August ( $1.51 \pm 0.21$ ). Such values are typical for fresh smoke measured in

Amazonian forest and African Savannas (e.g. Reid et al., 2005). In general, the monthly mean values of the Ångström exponent in Athens present their maxima on July and August (e.g. Gerasopoulos et al., 2011).

It has to be kept in mind that beyond smoke, local sources of anthropogenic pollution in the planetary boundary layer may have additionally contributed to the overall signal. Therefore, the measured columnar properties are attributed to a mixed aerosol state of smoke with anthropogenic pollution. However, Raman lidar measurements for August 22 in the free tropospheric region (considered unaffected by anthropogenic pollution), also revealed extinction and backscatter-related Ångström exponents, which ranged between 1.0 and 2.0 (Fig. 7). The lidar ratios from these measurements ranged between 70 and 90 sr, showing no wavelength dependence between 355 and 532 nm. The lidar-related values reported here, indicate typical properties of fresh smoke (e.g. Mueller et al., 2007). Values of the same order were retrieved for the columnar lidar ratio also by the AERONET inversion algorithm on August 23, when high AODs were accompanied by high Ångström values. These lidar ratios of the order of 78 sr at 440 nm, showed however a wavelength dependence, with a ratio of the lidar ratios between 440 and 870 nm to be of the order of 1.5. The reasons for this discrepancy are not yet fully understood and determined (see Mueller et al., 2007).

High values of the lidar ratios denote also the absorption nature of the fresh smoke particles. This behavior is evident when we examine the columnar absorption retrievals from the AERONET microphysical inversions. Specifically, on August 23 AERONET revealed a single scattering albedo (ssa) of 0.77 at 440 nm, at 05:07 UT, corresponding to the fresh smoke advection, while at 16:03 UT, the ssa reached 0.84. The ssa value of 0.77 is consistent with the one reported by Reid et al. (2005) for fresh smoke from flaming scrub forest fires. Moreover, the vegetation type is consistent with the source examined here according to the burnt scar mapping presented in Fig. 1.

#### 4.2. Aerosol radiative impact

The smoke aerosol load over Athens had a strong impact on surface radiation fields. The erythemal irradiance measured by the Brewer spectroradiometer is shown in Fig. 8a. During August 22, the plume was directed toward the station from the morning until

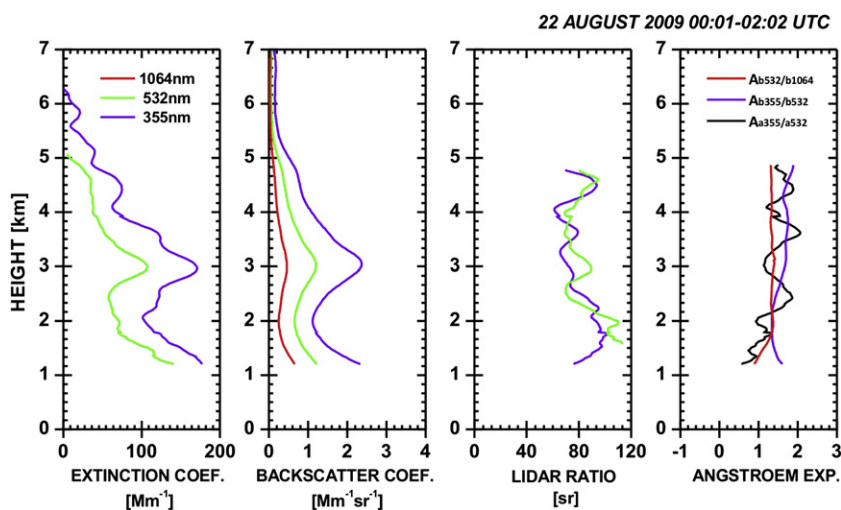


**Fig. 7.** 2-h mean lidar profiles on August 22 (00:01–02:02 UTC) of (a) aerosol extinction coefficients at 355 and 532 nm, (b) aerosol backscatter coefficients at 355, 532 and 1064 nm, (c) lidar ratio at 355 and 532 nm, and (d) backscatter-related (532/1064 and 355/532) and extinction-related (355/532) Ångström exponents.

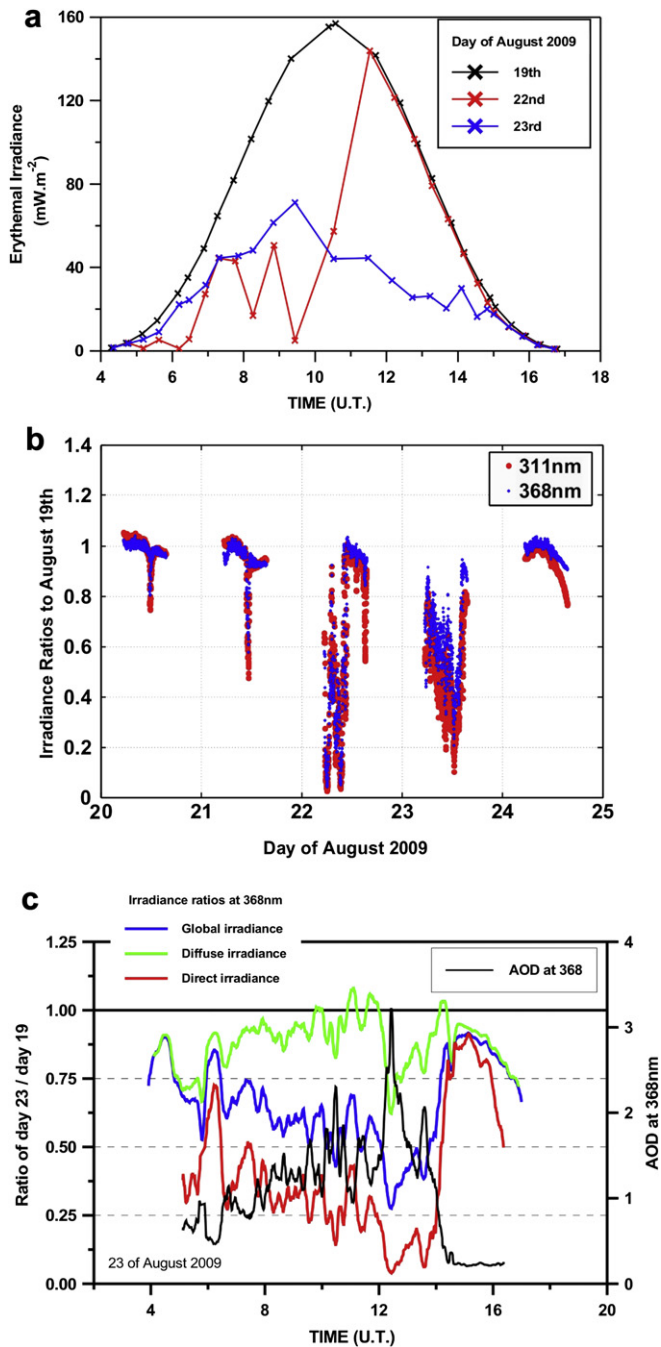


**Fig. 8.** (a) Erythemal dose measured by the Brewer spectroradiometer, (b) Global irradiance (UV-B and UVA) ratios for each fire event day to August 19, (c) Diurnal pattern of AOD at 368 nm for August 23 (black) and global, diffuse and direct irradiance ratios at 368 nm for August 23 to August 19.

12:00 UTC. Then, due to the change of the wind direction, solar irradiance was practically unaffected by the plume compared to August 19, as the direct sun optical path was clear. On August 23, the smoke was above the station for the whole day, resulting in a reduction of the erythemal irradiance from 160 to 40 mW m<sup>-2</sup>. Similar results were reported from the UV-MFR irradiance data (UV-B and UVA wavelengths). To understand the wavelength dependence of the aerosol effect on UV irradiance, 1-min ratios of the irradiances for days 20–24, in respect to the ones recorded on cloudless August 19, are shown in Fig. 8b. Ratios shown here correspond to the same solar zenith angles. During August 22 and

23, reductions up to 95% and 80% were found, respectively, for UVA global irradiances. Comparing UV-B (311 nm) and UVA (368 nm) results, it is shown that the reduction in the UV-B irradiance is stronger. This is due to the enhanced aerosol scattering at lower wavelengths, which absorbs radiation at 311 nm wavelength.

Looking such ratios in more detail, independently for global, diffuse and direct solar irradiance measurements (Fig. 8c), the reduction of the different irradiance components on August 23 is shown for together with the calculated AOD during this day. The smoke effect in the direct component on August 23, showed maximum reductions in the range of 30% up to 95%. The diffuse irradiance shows smaller reduction (about 20% on average) during that day. The contribution of the two components in the global irradiance reduction depends on the solar zenith angle, as around noon the direct contribution to the global irradiance reaches a maximum (due to the shorter optical path), thus the total reduction in the global irradiance is higher. Investigating the diffuse-global and direct UV reduction due to AOD variability, we have calculated the anti-correlation of each component reduction with the normalized (with the cosine of solar zenith angle) AOD (AODn), in order to consider the effect of the optical path. Results showed that Diffuse/Global/Direct irradiance reduction at 368 nm had a rate of -10.1%/-21.0%/-32.2% per unit of AODn, respectively, taking into account the AOD changes for the specific day. It is worth to note that for the whole period clouds were absent, so the reduction of the solar irradiance was purely due to aerosols (local background plus fire event).

#### 4.3. Impact on surface aerosol levels and air pollutants

To study the impact of the smoke plume on surface air quality, three different groups of stations, depending on the distance from

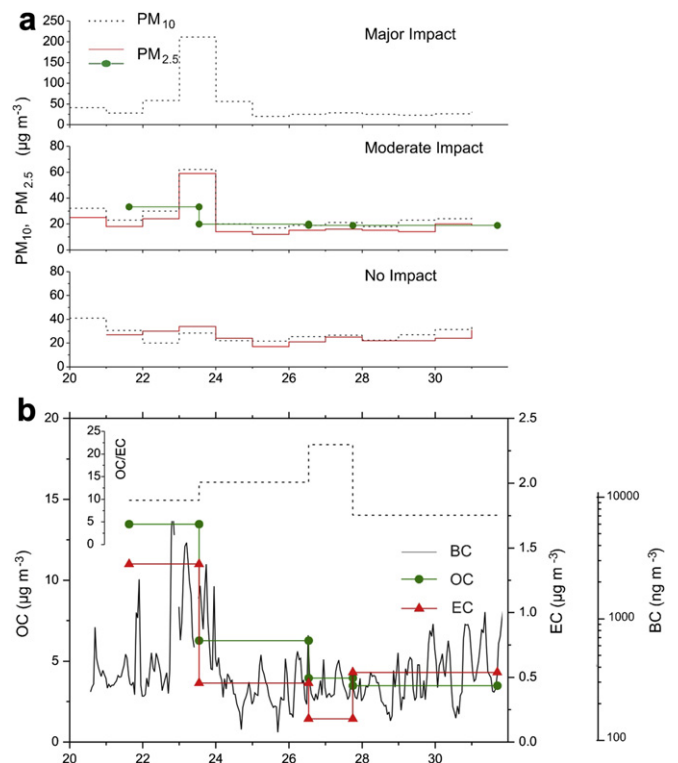


**Fig. 9.** (a) PM<sub>2.5</sub> and PM<sub>10</sub> surface concentrations in Athens. Stations are grouped as i. major impact (Koropi), ii. moderate impact (Ag. Paraskevi, Demokritos) and iii. no impact (Marousi, Lykovrisi, Thrakomakedones), depending on the distance from the plume path. (b) EC and OC concentrations from PM<sub>2.5</sub> filter sampling at Demokritos station, and concurrent BC measurements. The ratio OC/EC is also included in the internal panel.



the plume path are chosen. Koropi station is located near the centerline of the plume and is classified here as “major impact”. Ag. Paraskevi and Demokritos stations are located at a distance of about 3 km perpendicular to the plume axis and to the west, characterized as “moderate impact”. Finally, Marousi-Lykovrisi-Thrakomakedones stations were not affected by the smoke plume (located at distances in the range 7–12 km perpendicular to the plume axis to the west) and are characterized as “no impact”. For the “no impact” stations a total average for each parameter was extracted, since no significant deviation in pollutant levels was measured.

Regarding PM<sub>10</sub>, the urban background level during the period of study, as drawn from the “no impact” stations (Fig. 9a), is about 30  $\mu\text{g m}^{-3}$ , while for PM<sub>2.5</sub> it is about 25  $\mu\text{g m}^{-3}$ . At the “major impact” station, PM<sub>10</sub> levels showed a marked increase on August 23 as high as 210  $\mu\text{g m}^{-3}$ , while relative enhanced levels (60  $\mu\text{g m}^{-3}$ ) are also encountered on August 22 and 24. At the “moderate impact” station, PM<sub>10</sub> showed an increase from 30  $\mu\text{g m}^{-3}$  to 62  $\mu\text{g m}^{-3}$ , and at the same time PM<sub>2.5</sub> rose from 24  $\mu\text{g m}^{-3}$  to 59  $\mu\text{g m}^{-3}$ , demonstrating the dominance of fine particles near the surface due to the fire plume. The PM<sub>2.5</sub> concentrations were also recorded at the

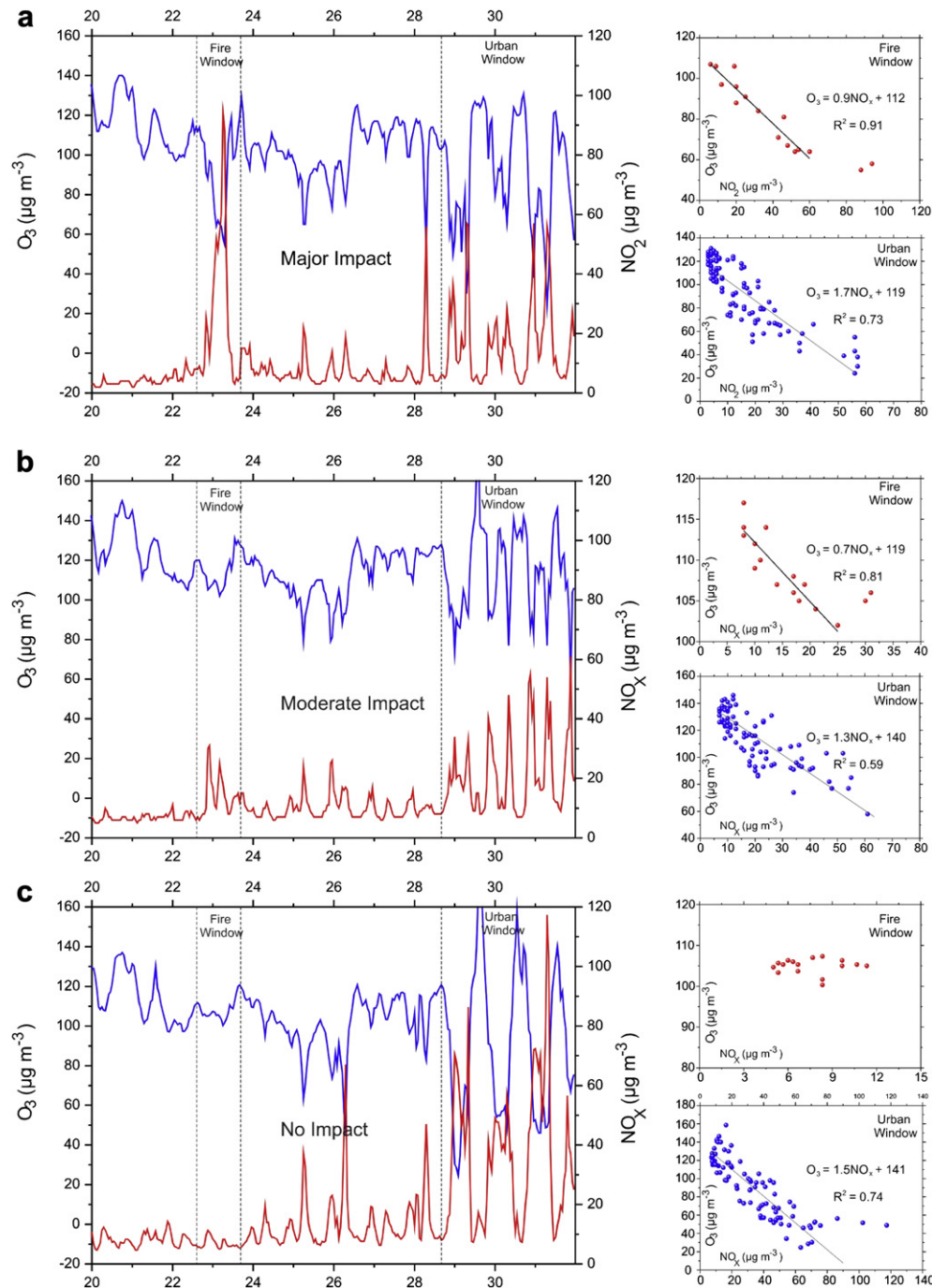


**Fig. 10.** O<sub>3</sub> and NO<sub>x</sub> surface concentrations in Athens. (a) major impact (Koropi), (b) moderate impact (Ag. Paraskevi, Demokritos) and (c) no impact (Marousi, Lykovrisi, Thrakomakedones), stations, depending on the distance from the plume path. In the right panels, scatter plots of O<sub>3</sub> vs. NO<sub>x</sub> are presented along with respective linear regressions, focusing on two time windows centered on the smoke episode and a typical period of urban photochemical processes.

“Demokritos” site at the basis of filter samples. The filter sampling during August 22 and part of 23 presents a value of  $33 \mu\text{g m}^{-3}$ , which coincides the same period average at Ag. Paraskevi.

To identify the signature of the fire on the chemical composition of surface aerosols, and in particular at the dominant  $\text{PM}_{2.5}$  fraction, the filters were analyzed for OC and EC. In Fig. 9b, it is shown that on August 22 and 23 both OC and EC presented large values, 13.5 and  $1.4 \mu\text{g m}^{-3}$ , respectively, compared to average site levels, in the order of 2–4 and  $0.5\text{--}1 \mu\text{g m}^{-3}$  (unpublished data), but also to the days after the fire episode. To overcome the different temporal resolution of the filter samplings compared to the rest of the stations, we have additionally plotted continuous measurements of BC. It is evident that the major impact is encountered on the evening of August 22 and during August 23, in slight delay with the signal captured from the columnar measurements.

Compared to other anthropogenic sources, during forest fires, more OC than EC is emitted, resulting in a relatively higher OC/EC ratio (Gelencsér et al., 2007; Watson et al., 2001). During the 2003 intense forest fires in Portugal, the OC/EC ratio was up to 7, compared to baseline periods, when it has values around 3 (Pio et al., 2008). At “Demokritos” site the average OC/EC ratio is about 4 (unpublished data) and during the case study (Fig. 9b, internal panel) it ranged between 10 and 14. An even higher value of the ratio (22) during the following days is due to the unusually low concentration of EC.

The impact of the smoke plume was also observed in the gaseous phase. In-situ air quality measurements show a remarkable temporal and spatial variability, demonstrating the impact of smoke on local air quality and photochemical processes. Our analysis of  $\text{O}_3$  and  $\text{NO}_x$  ( $\text{NO}_2 + \text{NO}$ ) measurements presented in Fig. 10, focuses on two time windows centered around the smoke episode and a typical period of urban photochemical processes. It has to be kept in mind that during August, habitants of Athens are taking their vacations, therefore  $\text{NO}_x$  levels are low, while during their return (end of August) traffic emissions are evident.

At the “major impact” station,  $\text{NO}_x$  values gradually climbed from below  $10 \mu\text{g m}^{-3}$  to  $94 \mu\text{g m}^{-3}$  during the smoke episode starting on August 22, while at the same time  $\text{O}_3$  decreased by  $50 \mu\text{g m}^{-3}$ . The timing of these changes, initially with the absence of active photochemical processes, demonstrates  $\text{NO}_x$  emissions from the fire, which gave rise to ozone removal through the process of titration (reaction of  $\text{O}_3$  with  $\text{NO}$  to  $\text{NO}_2$  and  $\text{O}_2$ ). At the “moderate impact” station,  $\text{NO}_x$  peaked at about  $30 \mu\text{g m}^{-3}$ , while  $\text{O}_3$  still anti-correlated with  $\text{NO}_2$ , presented a slighter decrease. Finally, no changes that could be attributed to the fire were observed in the “no impact” sites, a fact serving as reference for the impact of the fire plume on the local air quality levels and processes.

To this direction, the slope of  $\text{O}_3$  vs.  $\text{NO}_x$  during the presence of the smoke plume and during the traffic activity period (right panels of Fig. 10), was additionally investigated for the three different impacted types. It is evident that in both “major” and “moderate” smoke impact stations, the slopes (0.7–0.9) indicate direct and almost 1:1  $\text{NO}_x$  titration of  $\text{O}_3$ , while the respective slopes for traffic conditions are much higher (1.3–1.7), indicating more complex photochemical processes. In all cases, the reduction of solar irradiance and consequently of  $\text{O}^1\text{D}$  and  $\text{NO}_2$  photolysis rates is considered as an additional possible factor that affects  $\text{O}_3\text{--NO}_x$  photochemistry.

## 5. Summary and conclusions

Fires burning near urban environments may produce particularly dense pollution plumes that carry a mixture of anthropogenic and biomass burning pollutants and result in chemical processes that are different from those within pure biomass burning or pure anthropogenic pollution environments. In this paper, the temporal

evolution of the major pollutants, at different distances from the plume, is presented, in order to demonstrate the effect of primary fire emissions at a typical urban environment. The synergy of ground-based lidar, sunphotometric and surface measurements of particulate and air pollutants allowed estimating key characteristics of the smoke observed over Athens. These results are important (a) for aerosol characterization, (b) for the interpretation and improvement of satellite retrievals, (c) for radiative transfer calculations and (d) deeper investigation of chemical processes. The above are rather crucial for the region under study, both for aerosol radiative forcing of absorbing smoke and the effects on the photochemical activity (e.g. Zerefos et al., 2002).

Interesting features for 2009 Athens’ fires are here demonstrated for the first time: Lidar measurements showed that the smoke plume was distributed homogeneously within the PBL of Athens, reaching in cases free tropospheric heights (2–4 km). Both columnar aerosol retrievals and surface measurements revealed the dominance of fine over coarse mode. The absorbing characteristics of the smoke plume were identified, as high concentration levels of both EC and OC, leading to low values of the columnar single scattering albedo, typical for fresh smoke. Emission of  $\text{NO}_x$  from the fires had a direct and almost 1:1 impact on  $\text{O}_3$  concentrations, indicating different photochemical processes than normal. The reduction of solar irradiance, found to be of the order of 70%, which is considered as an additional possible factor that affected  $\text{O}_3\text{--NO}_x$  photochemistry.

Forest fires occurring near highly populated cities are of particular concern since they add to the impacts caused by high urban pollution levels. Further elaboration on the processes taking place during similar fire events near urban centers could make use of the results presented in this paper. The knowledge of the optical properties of smoke in this region is very important for climatic studies, taking also into account the increasing trend of forest fires during the last decade, mostly due to prolonged dry summers.

## Acknowledgments

The authors would like to acknowledge the NASA/AERONET team for data distribution. We also acknowledge the MODIS mission scientists and associated NASA personnel for the production of the data used. The research leading to these results has received partial funding from the following EU FP6 and FP7 projects: CITYZEN (FP7/2007–2013, grant agreement no 212095); MEGAPOLI (FP/2007–2011, grant agreement no 212520); SAFER (FP7/2007–2013, grant agreement no 218802); ENSEMBLES (FP6, GOCE-CT-2003-505539); ACI-UV (FP7-PEOPLE-2009-RG Marie Curie European Reintegration Grant, PERG05-GA-2009-247492); PARTHENO2N (FP7-PEOPLE-2009-RG Marie Curie European Reintegration Grant, PERG-GA-2009-256391).

## References

- Amiridis, V., Balis, D.S., Kazadzis, S., Bais, A., Giannakaki, E., Papayannis, A., Zerefos, C., 2005. Four-year aerosol observations with a Raman lidar at Thessaloniki, Greece, in the framework of European aerosol research lidar network (EARLINET). *J. Geophys. Res.* 110, D21203. doi:10.1029/2005JD006190.
- Amiridis, V., Balis, D.S., Giannakaki, E., Stohl, A., Kazadzis, S., Koukoulis, M.E., Zanis, P., 2009a. Optical characteristics of biomass burning aerosols over Southeastern Europe determined from UV-Raman lidar measurements. *Atmos. Chem. Phys.* 9, 2431–2440.
- Amiridis, V., Kafatos, M., Perez, C., Kazadzis, S., Gerasopoulos, E., Mamouri, R.E., Papayannis, A., Kokkalis, P., Giannakaki, E., Basart, S., Daglis, I., Zerefos, C., 2009b. The potential of the synergistic use of passive and active remote sensing measurements for the validation of a regional dust model. *Ann. Geophys.* 27, 3155–3164.
- Balis, D., Amiridis, V., Zerefos, C., Gerasopoulos, E., Andreae, M.O., Zanis, P., Kazantzidis, A., Kazadzis, S., Papayannis, A., 2003. Raman lidar and sunphotometric measurements of aerosol optical properties over Thessaloniki, Greece, during a biomass burning episode. *Atmos. Environ.* 37 (32), 4529–4538.



- Crutzen, P.J., Andreae, M.O., 1990. Biomass burning in the tropics: impacts on atmospheric chemistry and biogeochemical cycles. *Science* 250 (4988), 1669–1678.
- Forster, P., et al., 2007. Changes in atmospheric constituents and in radiative forcing. In: Solomon, S., Qin, D., Manning, M., Chen, Z., Marquis, M., Averyt, K.B., Tignor, M., Miller, H.L. (Eds.), *Climate Change 2007: The Physical Science Basis. Contribution of Working Group I to the Fourth Assessment Report of the Intergovernmental Panel on Climate Change*. Cambridge University Press, Cambridge, United Kingdom and New York, NY, USA.
- Founda, D., Giannakopoulos, C., 2009. The exceptionally hot summer of 2007 in Athens, Greece – A typical summer in the future climate? *Glob. Planet. Change* 67, 227–236.
- Gelencsér, A., May, B., Simpson, D., Sanchez-Ochoa, A., Kasper-Giebl, A., Puxbaum, H., Caseiro, A., Pio, C., Legrand, M., 2007. Source apportionment of PM<sub>2.5</sub> organic aerosol over Europe: primary/secondary, natural/anthropogenic, fossil/biogenic origin. *J. Geophys. Res.* 112, D23S04. doi:10.1029/2006JD008094.
- Gerasopoulos, E., Amiridis, V., Kazadzis, S., Kokkalis, P., Eleftheratos, K., Andreae, M.O., Andreae, T.W., El-Askary, H., Zerefos, C.S., 2011. Three-year ground based measurements of aerosol optical depth over the Eastern Mediterranean: the urban environment of Athens. *Atmos. Chem. Phys.* 11, 2145–2159. doi:10.5194/acp-11-2145-2011.
- Giannakopoulos, C., Kostopoulou, E., Varotsos, K.V., Tziotziou, K., Plitharas, A., 2011. An integrated assessment of climate change impacts for Greece in the near future. *Reg. Environ. Change*. doi:10.1007/s10113-011-0219-8.
- Giannakopoulos, C., Le Sager, P., Bindi, M., Moriondo, M., Kostopoulou, E., Goodess, C.M., 2009. Climatic changes and associated impacts in the Mediterranean resulting from a 2 °C Global Warming. *Glob. Planet. Change* 68, 209–224.
- Giglio, L., Descloitres, J., Justice, C.O., Kaufman, Y.J., 2003. An enhanced contextual fire detection algorithm for MODIS. *Remote Sens. Environ.* 87, 273–282. doi:10.1016/S0034-4257(03)00184-6.
- Grivas, G., Chaloukakou, A., Kassomenos, P., 2008. An overview of the PM<sub>10</sub> pollution problem, in the Metropolitan area of Athens, Greece. Assessment of controlling factors and potential impact of long range transport. *Sci. Total Environ.* 389, 165–177. doi:10.1016/j.scitotenv.2007.08.048.
- Harrison, L., Michalsky, J., 1994. Objective algorithms for the retrieval of optical depths from ground-based measurements. *Appl. Opt.* 33, 5126–5132.
- Holben, B.N., Eck, T.F., Slutsker, I., Tanre, D., Buis, J.P., Setzer, A., Vermote, E., Reagan, J.A., Kaufman, Y.J., Nakajima, T., Lavenu, F., Jankowiak, I., Smirnov, A., 1998. AERONET-A federated instrument network and data archive for aerosol characterization. *Remote Sens. Environ.* 66 (1), 1–16. doi:10.1016/S0034-4257(98)00031-5.
- Karanasidou, A.A., et al., 2009. Assessment of source apportionment by positive matrix factorization analysis on fine and coarse urban aerosol size fractions. *Atmos. Environ.* 43, 3385–3395. doi:10.1016/j.atmosenv.2009.03.051.
- Kazadzis, S., Bais, A., Amiridis, V., Balis, D., Meleti, C., Kouremeti, N., Zerefos, C.S., Rapsomanikis, S., Petrakakis, M., Kelesis, A., Tzoumaka, P., Kelektsoyglou, K., 2007. Nine years of UV aerosol optical depth measurements at Thessaloniki, Greece. *Atmos. Chem. Phys.* 7, 2091–2101.
- Kontoes, C.C., 2008. Operational land cover change detection using change-vector analysis. *Int. J. Remote Sensing* 29 (No. 16), 4757–4779. doi:10.1080/01431160801961367.
- Liu, Y., Kahn, R., Chaloulakou, A., Koutrakis, P., 2009. Analysis of the impact of the forest fires in August 2007 on air quality of Athens using multi-sensor aerosol remote sensing data, meteorology, and surface observations. *Atmos. Environ.* doi:10.1016/j.atmosenv.2009.04.010.
- Mamouri, R.E., Amiridis, V., Papayannis, A., Giannakaki, E., Tsaknakis, G., Balis, D., 2009. Validation of CALIPSO space-borne derived attenuated backscatter coefficient profiles using a ground-based lidar in Athens, Greece. *Atmos. Measurements Tech.* 2, 513–522.
- Markowicz, K.M., Flatau, P.J., Ramana, M.V., Crutzen, P.J., Ramanathan, V., 2002. Absorbing Mediterranean aerosols lead to a large reduction in the solar radiation at the surface. *Geophys. Res. Lett.* doi:10.1029/2002GL015767.
- Matthias, V., Freudenthaler, V., Amodeo, A., Balin, I., Balis, D., Bosenberg, J., Chaikovskiy, A., Chourdakis, G., Comeron, A., Delaval, A., de Tomasi, F., Eixmann, R., Hagard, A., Komguem, L., Kreipl, S., Matthey, R., Rizi, V., Rodrigues, J.A., Wandinger, U., Wang, X., 2004. Aerosol lidar intercomparison in the framework of EARLINET project. 1. Instruments. *Appl. Opt.* 43, 961–976.
- Mueller, D., Ansmann, A., Mattis, I., Tesche, M., Wandinger, U., Althausen, D., Pisani, G., 2007. Aerosol-type-dependent lidar ratios observed with Raman lidar. *J. Geophys. Res.* 112, D16202. doi:10.1029/2006JD008292.
- Pappalardo, G., Amodeo, A., Pandolfi, M., Wandinger, U., Ansmann, A., Bösenberg, J., Matthias, V., Amiridis, V., De Tomasi, F., Frioud, M., Iarlori, M., Komguem, L., Papayannis, A., Rocadenbosch, F., Wang, X., 2004. Aerosol lidar intercomparison in the framework of EARLINET: part III – Raman lidar algorithm for aerosol extinction, backscatter and lidar ratio. *Appl. Opt.* 43, 5370–5385.
- Pio, C.A., Alves, C.A., Oliveira, T., Afonso, J., Caseiro, A., Puxbaum, H., Kasper-Giebl, A., Preunkert, S., Legrand, M., Gelencsér, A., 2008. Composition and source apportionment of atmospheric aerosols in Portugal during the 2003 summer intense forest fire period. *Atmos. Environ.* 42, 7530–7543.
- Prezerakos, N.G., 1984. Does the extension of the Azores anticyclone towards the Balkans really exist. *Arch. Meteorol. Geophys. Bioklimatol Ser. A* 33, 217–227.
- Reid, J.S., et al., 2005. A review of biomass burning emissions part III: intensive optical properties of biomass burning particles. *Atmos. Chem. Phys.* 5, 827–849.
- Richter, A., Burrows, J.P., 2002. Tropospheric NO<sub>2</sub> from GOME measurements. *Adv. Space Res.* 29 (11), 1673–1683.
- Sciare, J., Oikonomou, K., Favez, O., Liakakou, E., Markaki, Z., Cachier, H., Mihalopoulos, N., 2008. Long-term measurements of carbonaceous aerosols in the Eastern Mediterranean: evidence of long-range transport of biomass burning. *Atmos. Chem. Phys.* 8, 5551–5563.
- Seiler, W., Crutzen, P.J., 1980. Estimates of gross and net fluxes of carbon between the biosphere and atmosphere from biomass burning. *Clim. Change* 2, 207–247.
- Stohl, A., Berg, T., Burkhardt, J.F., Fjærraa, A.M., Forster, C., Herber, A., Hov, Ø., Lunder, C., McMillan, W.W., Oltmans, S., Shiobara, M., Simpson, D., Solberg, S., Stebel, K., Ström, J., Tørseth, K., Treffeisen, R., Virkkunen, K., Yttri, K.E., 2007. Arctic smoke – record high air pollution levels in the European Arctic due to agricultural fires in Eastern Europe. *Atmos. Chem. Phys.* 7, 511–534.
- Stohl, A., Forster, C., Frank, A., Seibert, P., Wotawa, G., 2005. Technical Note: the Lagrangian particle dispersion model FLEXPART version 6.2. *Atmos. Chem. Phys.* 5, 2461–2474.
- Turquety, S., Hurtmans, D., Hadji-Lazaro, J., Coheur, P.F., Clerbaux, C., Josset, D., Tsamalis, C., 2009. Tracking the emission and transport of pollution from wildfires using the IASI CO retrievals: analysis of the summer 2007 Greek fires. *Atmos. Chem. Phys.* 9, 4897–4913. doi:10.5194/acp-9-4897-2009.
- Valks, P., Pinardi, G., Richter, A., Lambert, J.-C., Hao, N., Loyola, D., Van Roozendael, M., Emmadi, S., 2011. Operational total and tropospheric NO<sub>2</sub> column retrieval for GOME-2. *Atmos. Meas. Tech. Discuss.* 4, 1617–1676. doi:10.5194/amtd-4-1617-2011.
- Watson, J.G., Chow, J.C., Houck, J.E., 2001. PM<sub>2.5</sub> chemical source profiles for vehicle exhaust, vegetative burning, geological material, and coal burning in North-western Colorado during 1995. *Chemosphere* 43, 1141–1151.
- Zerefos, C.S., Kourtidis, K.A., Melas, D., Balis, D., Zanis, P., Mantis, H.T., Repapis, C., Isaksen, I., Sundet, J., Herman, J., Bhartia, P.K., Calpini, B., 2002. Photochemical activity and solar ultraviolet radiation modulation factors (PAUR): an overview of the project. *J. Geophys. Res.* doi:10.1029/2000JD000134.
- Zerefos, C.S., Eleftheratos, K., 2007. The Atmospheric Environment Division of the Center of Environmental Health & Biophysics of the Biomedical Research Foundation of the Academy of Athens, in Bio Academy, A Quarterly Bulletin of the Biomedical Research Foundation. Academy of Athens, Issue 1, 10–13 pp.